



HAL
open science

IMPACT OF GENERALIZED GROWTH DYNAMICS AND SPATIAL DISPERSAL ON MAXIMUM SUSTAINABLE YIELD IN HARVESTED POPULATIONS

Bilel Elbetch, Ali Moussaoui

► **To cite this version:**

Bilel Elbetch, Ali Moussaoui. IMPACT OF GENERALIZED GROWTH DYNAMICS AND SPATIAL DISPERSAL ON MAXIMUM SUSTAINABLE YIELD IN HARVESTED POPULATIONS. 2025. <hal-05085735>

HAL Id: hal-05085735

<https://hal.science/hal-05085735v1>

Preprint submitted on 26 May 2025

HAL is a multi-disciplinary open access archive for the deposit and dissemination of scientific research documents, whether they are published or not. The documents may come from teaching and research institutions in France or abroad, or from public or private research centers.

L'archive ouverte pluridisciplinaire **HAL**, est destinée au dépôt et à la diffusion de documents scientifiques de niveau recherche, publiés ou non, émanant des établissements d'enseignement et de recherche français ou étrangers, des laboratoires publics ou privés.



HAL Authorization

22 **1. Introduction.** The growth and dynamics of populations are influenced by a multitude
 23 of factors, among which dispersal plays a critical role. Dispersal, which can occur in
 24 varying amounts and often in random patterns, has significant implications for ecosystems.
 25 It can disrupt ecological balances, influence the persistence or extinction of species, and
 26 reshape the structure of communities. The importance of dispersal in population dynamics
 27 has been extensively studied, with foundational insights provided by Allen in works such
 28 as [1, 2, 3] and further explored by Holt in [44]. These studies highlight the complex
 29 interplay between dispersal and ecosystem stability, offering valuable perspectives on how
 30 movement patterns affect ecological outcomes.

31 In [1], Allen considered the n -patch general model given by the following equations:

$$\frac{dx_i}{dt} = x_i(a_i - b_i x_i) + \varepsilon \Upsilon_i(x), \quad i = 1, \dots, n, \quad (1.1)$$

32 where a_i and b_i are positive constants; $x = (x_1, \dots, x_n)^T$, where x_i represents the population
 33 density in the i -th patch. The parameter ε is the dispersal rate. The function Υ_i represents
 34 one of three different mechanisms. The mechanism for linear diffusion is given by:

$$\Upsilon_i(x) = \sum_{j=1, j \neq i}^n D_{ij}(x_j - \alpha_{ij} x_i), \quad i = 1, \dots, n, \quad (1.2)$$

35 where D_{ij} and α_{ij} are positive constants. Dispersal by linear diffusion implies that the
 36 species is able to move to all locations within its environment with equal probability. The
 37 mechanism for biased diffusion is given by:

$$\Upsilon_i(x) = \sum_{j=1, j \neq i}^n D_{ij} x_i (x_j - \alpha_{ij} x_i), \quad i = 1, \dots, n, \quad (1.3)$$

38 Note that the term "biased" means that the diffusion rate is a function of population density.
 39 The diffusion rate is regulated by population density, increasing for large populations and
 40 decreasing for small populations. The third type of mechanism is the directed diffusion,
 41 which was formulated by Gurney and Nisbet [42], and is given by:

$$\Upsilon_i(x) = \sum_{j=1, j \neq i}^n D_{ij}(x_j^2 - \alpha_{ij} x_i^2), \quad i = 1, \dots, n, \quad (1.4)$$

42 Dispersal by directed diffusion implies that individuals move from regions of high popula-
 43 tion density to regions of low density, i.e., movement is a function of species density. For
 44 more details on the biological interpretation and the continuous formulation of such types of
 45 diffusion, we refer the reader to [1]. One particularly interesting case of system (1.1) is that
 46 of *perfect mixing*, which occurs when the migration rate ε tends to infinity—in other words,
 47 when there are no constraints on movement (see [20, 21, 22, 23, 24, 25, 26, 27, 28, 29] for
 48 further examples and details).

49 The objective of the work by Allen [1] is to study the effect of different types of dispersal
 50 on the persistence and extinction of species. The persistence and extinction behavior is
 51 completely determined in the two-patch model (1.1)(1.2) for $n = 2$ (see Theorem 1 in [1]).
 52 For model (1.1)(1.3), Allen [1, Theorem 2] showed that a population subject to biased
 53 diffusion is always persistent and, in fact, represents a strongly persistent population. For
 54 more details on persistence and extinction results, see Theorem 3 of [1] for the n -patch

55 model (1.1)(1.3), Theorem 4 of [1] for the n -patch model (1.1)(1.4), and Proposition 1
56 of [1] for the two-patch case.

57 Dispersal plays a crucial role in population dynamics, influencing both local popula-
58 tion densities and overall resource availability. In a multi-patch fishery model, individuals
59 migrate between patches in response to ecological factors such as resource abundance, en-
60 vironmental conditions, and intra-specific competition. While migration can enhance pop-
61 ulation persistence and resilience, it may also lead to unintended consequences for yield
62 optimization. Therefore, understanding how dispersal patterns influence the maximum
63 sustainable yield (MSY) is essential for the development of effective fisheries management
64 strategies.

65 Most recent mathematical models take into account the spatial distribution of fish-
66 eries to study the management of multi-patch systems [5, 11, 43, 50, 51, 52], as well as
67 prey–predator models in a multi-patch environment [31, 53], and Gradostat models [32].
68 One fundamental principle in fisheries management is the concept of the maximum sus-
69 tainable yield (MSY), which refers to the largest amount of fish that can be harvested from
70 a population without compromising its long-term sustainability. Determining MSY is key
71 to achieving the objective of harvesting as many fish as possible without risking population
72 collapse [15].

73 There is considerable interest in understanding how spatial heterogeneity influences the
74 MSY of multi-site systems connected through dispersal or migration. This raises a cen-
75 tral question: how does connectivity among fishing sites affect fishery productivity? For
76 instance, can the MSY of a fishery be increased by linking fishing sites through migratory
77 flows—and if so, to what extent does heterogeneity play a role?

78 The answer is not straightforward. In the case of two fishing sites connected by rapid
79 migrations and focusing on a single harvested species, the MSY of the connected system
80 does not exceed the sum of the MSYs of the isolated sites. However, in a prey–predator
81 context, where the predator is a commercially harvested species and the prey is unhar-
82 vested, the situation is different. In this case, the MSY of the predator in the connected
83 system can indeed exceed the sum of the MSYs obtained when the two sites are managed
84 independently.

85 This phenomenon can be summarized as follows:

$$MSY(\varepsilon \rightarrow \infty) > MSY_1(\varepsilon \rightarrow 0) + MSY_2(\varepsilon \rightarrow 0).$$

86 This result was first established in [4] for a system consisting of two fishing sites connected
87 by fast migration, and is described by the following model:

$$\begin{cases} \frac{dx_1}{d\tau} = \varepsilon \left[r_1 x_1 \left(1 - \frac{x_1}{K_1} \right) - E x_1 \right] + \gamma_{12} x_2 - \gamma_{21} x_1, \\ \frac{dx_2}{d\tau} = \varepsilon \left[r_2 x_2 \left(1 - \frac{x_2}{K_2} \right) - E x_2 \right] + \gamma_{21} x_1 - \gamma_{12} x_2, \end{cases} \quad (1.5)$$

88 where $\varepsilon \rightarrow 0$. Furthermore, we also refer to the work [14], in which this result was extended
89 to the case of a single species with variable fishing effort in a multi-site fishery involving
90 an arbitrary number of sites (not limited to two). In this latter study, since the fishing effort
91 is variable, the optimization of the harvest is carried out under a cost constraint, assuming
92 identical fishing operating costs across all sites.

93 In 2025, Pierre et al. [6] considered a multi-site fishery model with a single harvested
94 fish species and site-specific fishing efforts, described by the following system:

$$\frac{dx_i}{dt} = \varepsilon \left(r_i x_i \left(1 - \frac{x_i}{K_i} \right) - q E_i x_i \right) + \sum_{j=1, j \neq i}^n (\gamma_{ij} x_j - \gamma_{ji} x_i), \quad i = 1, \dots, n. \quad (1.6)$$

95 For this model, they showed that the Maximum Sustainable Yield (MSY) of the multi-
 96 site network, when the sites are connected, is always less than or equal to the sum of the
 97 MSYs of the isolated sites. Equality occurs when the fish population is spatially distributed
 98 according to the Ideal Free Distribution (IFD), i.e.,

$$MSY(\varepsilon \rightarrow \infty) \leq MSY_1(\varepsilon \rightarrow 0) + \dots + MSY_n(\varepsilon \rightarrow 0).$$

99 Recently, Elbetch et al. [33] have generalized these results for all migration rates ε , i.e.
 100 they showed that the Maximum Sustainable Yield of the multi-site network is always less
 101 than or equal to the sum of the MSYs of the isolated sites for all rate of migration, i.e.,

$$MSY(\varepsilon) \leq MSY_1(\varepsilon \rightarrow 0) + \dots + MSY_n(\varepsilon \rightarrow 0), \quad \forall \varepsilon \geq 0.$$

102 The objective of the present work is to investigate the influence of generalized growth
 103 rates on the Maximum Sustainable Yield (MSY) in population dynamics, focusing on both
 104 single-species and multi-patch models with harvesting. The study aims to derive condi-
 105 tions for equilibrium stability and to obtain expressions for MSY under various growth
 106 models, including logistic, Richards, and Gompertz formulations, in order to understand
 107 how different intrinsic growth functions and harvesting efforts affect sustainable yields.

108 Furthermore, the analysis is extended to multi-patch environments where dispersal be-
 109 tween patches is considered, to explore how spatial connectivity and migration influence
 110 yield optimization. The theoretical results demonstrate that the total MSY in connected
 111 patches is always less than or equal to the sum of MSYs from the isolated patches, re-
 112 gardless of migration intensity. These conclusions are supported by numerical simulations,
 113 which illustrate the trade-offs between connectivity and sustainable harvesting.

114 The structure of this paper is organized as follows: The introduction provides an overview
 115 of various studies on single-species and multi-patch models, including population dynam-
 116 ics in connected patches and the concept of Maximum Sustainable Yield (MSY). Section 2
 117 presents fundamental results on the generalized logistic equation with harvesting and de-
 118 rives conditions for MSY. Section 3 examines specific growth models (logistic, Richards,
 119 Gompertz) and their MSY calculations. Section 4 extends the analysis to multi-patch envi-
 120 ronments, comparing MSY between connected and isolated patches, and investigates how
 121 migration rates affect total yield at MSY. Section 5 presents numerical simulations validat-
 122 ing the theoretical findings. Finally, Section 6 summarizes the key insights, emphasizing
 123 the trade-off between connectivity and sustainable yield, and discusses implications for
 124 ecological resource management.

125 **2. Generalized growth rate and MSY.** In this section, our goal is to prove several results
 126 concerning the generalized logistic equation with harvesting. Let us consider the single-
 127 species generalized logistic equation with harvesting, given by:

$$\frac{dx}{dt} = x\varphi(x) - Ex, \quad (2.1)$$

128 where E denotes the fishing effort, x represents the population density of the species, and
 129 $x\varphi(x)$ corresponds to the specific growth rate of the population. Since the specific growth
 130 rate may depend on the environment, we list the following hypotheses, which are standard
 131 in single-species models (see [35, 58]):

132 H1. All solutions of the initial value problem (2.1) exist, are unique, and can be continued
 133 for all positive times.

134 H2. $\varphi(0) > 0$, $\frac{d\varphi}{dx}(x) < 0$, there exists $K > 0$ such that $\varphi(K) = 0$, and $x\varphi(x) \rightarrow -\infty$ as
 135 $x \rightarrow +\infty$.

136 The generalized logistic growth model (2.1) with constant harvesting has two equilibria:
 137 $x^* = 0$ and $x^* = x^*(E)$ satisfying $\varphi(x^*(E)) = E$. Note that since φ is strictly decreasing,
 138 the equation $\varphi(x) = E$ has a unique solution if and only if $E < \varphi(0)$. The equilibrium
 139 $x^*(E)$, which is positive when $E < \varphi(0)$, is stable, while the trivial equilibrium $x^* = 0$ is
 140 unstable in this case. Otherwise, when $E \geq \varphi(0)$, the equilibrium $x^* = 0$ is stable.

141 **Remark 1.** As the function φ is strictly decreasing then the function $E \mapsto x^*(E)$ is also
 142 strictly decreasing, i.e. $\frac{dx^*}{dE}(E) < 0$ for all $0 < E < \varphi(0)$.

143 At the positive equilibrium, the harvesting rate is:

$$Y^*(E) = Ex^*(E) = \begin{cases} x^*(E)\varphi(x^*(E)) & \text{if } E < \varphi(0), \\ 0 & \text{else.} \end{cases} \quad (2.2)$$

The derivative of yield $Y^*(E)$ with respect to the fishing effort E is given by:

$$\frac{dY^*}{dE}(E) = E \frac{dx^*}{dE}(E) + x^*(E) =: \phi(E).$$

144 Therefore, $\frac{dY^*}{dE}(E) = 0$ if and only if $\phi(E) = 0$. We have $\phi(0) = x^*(0) = K > 0$ and
 145 $\phi(\varphi(0)) = \varphi(0) \frac{dx^*}{dE}(\varphi(0)) < 0$ and the function ϕ is continuous so there is at least E_{MSY}^*
 146 such that $\phi(E_{MSY}^*) = 0$. Hence, Y^* having a maximum for fishing effort E_{MSY}^* such that
 147 $x_{MSY}^* = x^*(E_{MSY}^*)$, and corresponding to the *Maximum Sustainable Yield* (MSY). The cor-
 148 responding yield Y_{MSY}^* is given by the following expression:

$$Y_{MSY}^* = E_{MSY}^* x_{MSY}^* = x^*(E_{MSY}^*) \varphi(x^*(E_{MSY}^*)). \quad (2.3)$$

149 Which can rewritten as follow:

$$Y_{MSY}^* = \max_{0 \leq x \leq K} x\varphi(x). \quad (2.4)$$

150 **3. Some examples.** In this section, we provide examples of growth rates: the logistic
 151 model, the Richards model, and the Gompertz model. For each model, we calculate the
 152 Maximum Sustainable Yield (MSY). We begin by outlining some key properties of these
 153 models.

154 The Gompertz model is characterized by its asymmetric growth curve, which makes it
 155 particularly useful for describing phenomena such as tumor growth, where the growth rate
 156 gradually slows down over time. Its formula is given by

$$x(t) = K \cdot e^{-\ln\left(\frac{K}{x_0}\right) \cdot e^{-rt}},$$

157 where K represents the carrying capacity (maximum population size), x_0 is the initial pop-
 158 ulation size, and r is the intrinsic growth rate. The Gompertz model is more flexible than
 159 the logistic model for describing asymmetric growth patterns, but it is less intuitive and
 160 slightly more complex to fit to data.

161 The logistic model, on the other hand, is widely used to describe population growth in
 162 environments with limited resources. Its formula is given by

$$x(t) = \frac{K}{1 + \left(\frac{K-x_0}{x_0}\right) \cdot e^{-rt}},$$

163 where the parameters K , x_0 , and r have the same meanings as in the Gompertz model. The
 164 logistic model produces a symmetric S-shaped (sigmoidal) curve with a clear inflection
 165 point, making it simple and intuitive to use. However, its assumption of symmetry around
 166 the inflection point limits its flexibility for modeling asymmetric growth patterns.

167 The Richards model generalizes the logistic model by introducing an additional shape
 168 parameter μ , which controls the asymmetry of the growth curve. Its formula is given by

$$x(t) = \frac{K}{\left(1 + \left(\frac{K-x_0}{x_0}\right) \cdot e^{-rt}\right)^{\frac{1}{\mu}}}.$$

169 This added parameter allows the Richards model to describe a wider range of growth pat-
 170 terns, including asymmetric curves, making it highly flexible. When $\mu = 1$, the Richards
 171 model reduces to the logistic model, highlighting its broader applicability. However, this
 172 flexibility comes at the cost of increased complexity in parameter estimation and model
 173 fitting.

174 In summary, the Gompertz model is well-suited for asymmetric growth patterns, such as
 175 tumor growth, while the logistic model is ideal for simpler, symmetric population growth
 176 scenarios. The Richards model offers the greatest flexibility, accommodating a variety of
 177 growth shapes, but is more complex to work with due to its additional parameter. The
 178 choice of model depends on the specific characteristics of the data and the phenomenon
 179 being studied.

180 **Example 1.** *Let us consider the single-species logistic equation with harvesting [54]:*

$$\frac{dx}{dt} = rx \left(1 - \frac{x}{K}\right) - Ex, \quad (3.1)$$

181 where r is the growth rate, K the carrying capacity, and E the fishing effort. We now aim to
 182 choose the harvesting effort E in order to maximize the total harvesting term. The logistic
 183 growth equation (3.1) with constant harvesting has two equilibria: $x = 0$ and

$$x^*(E) = K \left(1 - \frac{E}{r}\right),$$

184 which is positive when $E < r$. When $x^*(E) > 0$, it is stable and the trivial equilibrium
 185 $x^* = 0$ is unstable; otherwise, $x^* = 0$ is stable. At the positive equilibrium, the harvesting
 186 rate is:

$$Y^*(E) = Ex^*(E) = \begin{cases} EK \left(1 - \frac{E}{r}\right) & \text{if } E < r, \\ 0 & \text{otherwise.} \end{cases} \quad (3.2)$$

187 The yield $Y^*(E)$ is a negative parabola with respect to the fishing effort E , having a maxi-
 188 mum for $E_{MSY}^* = \frac{r}{2}$ corresponding to the MSY. The corresponding value of the stable non-
 189 trivial positive equilibrium x^* reads as follows:

$$x_{MSY}^* := x^*(E_{MSY}^*) = \left(1 - \frac{E_{MSY}^*}{r}\right) K = \frac{K}{2}. \quad (3.3)$$

190 And the corresponding yield Y_{MSY}^* is given by the following expression:

$$Y_{MSY}^* = E_{MSY}^* x_{MSY}^* = E_{MSY}^* K \left(1 - \frac{E_{MSY}^*}{r}\right) = \frac{rK}{4}. \quad (3.4)$$

On other hand, using (2.4) we obtain:

$$Y_{MSY}^* = \max_{0 \leq x \leq K} x\varphi(x) = \max_{0 \leq x \leq K} rx \left(1 - \frac{x}{K}\right) = \frac{rK}{4}.$$

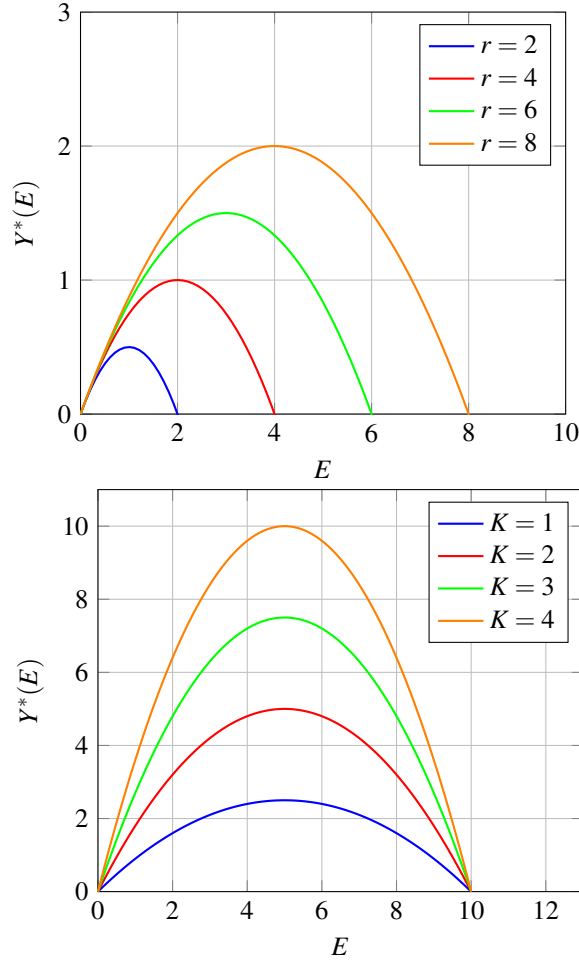


FIGURE 1. The function $Y(E) = EK \left(1 - \frac{E}{r}\right)$ for some values of r and K .

191 **Example 2.** Let us consider the single-species generalized logistic equation (model of
 192 Richards [22, 55]) with harvesting given by:

$$\frac{dx}{dt} = rx \left[1 - \left(\frac{x}{K}\right)^\mu\right] - Ex, \quad (3.5)$$

193 where r is the growth rate, K the carrying capacity, μ is a positive number, and E the
 194 fishing effort. We are now going to choose the harvesting effort E in order to maximize
 195 the total harvesting term. The generalized logistic growth (3.5) with constant harvesting

196 has two equilibria: $x^* = 0$ and $x^*(E) = K \left(1 - \frac{E}{r}\right)^{\mu^{-1}}$, which being positive when $E < r$.

197 When $x^*(E) > 0$, it is stable and the trivial equilibrium $x^* = 0$ is unstable and otherwise
 198 $x^* = 0$ is stable. At the positive equilibrium, the harvesting rate is:

$$Y^*(E) = Ex^*(E) = \begin{cases} EK \left(1 - \frac{E}{r}\right)^{\mu^{-1}} & \text{if } E < r, \\ 0 & \text{else.} \end{cases} \quad (3.6)$$

199 The yield $Y^*(E)$ having a maximum for $E_{MSY}^* = \frac{\mu}{\mu+1}r$ corresponding to the MSY, see figure 2. The corresponding value of the stable non-trivial positive equilibrium x^* reads as
 200 follows:
 201

$$x_{MSY}^* := x^*(E_{MSY}^*) = \left(1 - \frac{E_{MSY}^*}{r}\right)^{\mu-1} K = \left(\frac{1}{\mu+1}\right)^{\mu-1} K. \quad (3.7)$$

202 And the corresponding yield Y_{MSY}^* is given by the following expression:

$$Y_{MSY}^* = E_{MSY}^* x_{MSY}^* = E_{MSY}^* K \left(1 - \frac{E_{MSY}^*}{r}\right)^{\mu-1} = \mu \left(\frac{1}{\mu+1}\right)^{\mu-1+1} rK. \quad (3.8)$$

On other hand, using (2.4) we obtain:

$$Y_{MSY}^* = \max_{0 \leq x \leq K} x\varphi(x) = \max_{0 \leq x \leq K} rx \left[1 - \left(\frac{x}{K}\right)^\mu\right] = \mu \left(\frac{1}{\mu+1}\right)^{\mu-1+1} rK.$$

Note that, the function $\mu \mapsto Y_{MSY}^*(\mu)$ is increasing, indeed, its derivative is given by:

$$\frac{dY_{MSY}^*}{d\mu}(\mu) = -2 \left((\mu+1)^{-1}\right)^{\frac{\mu+1}{\mu}} \ln \left((\mu+1)^{-1}\right) \mu^{-1},$$

203 which is positive for all $\mu > 0$. For $\mu = 1$, the yield value is the MSY is achieved when the
 204 fishing effort E is chosen to be equal to half of the growth rate r of the harvested population,
 205 and the yield Y_{MSY}^* is becomes $\frac{rK}{4}$ (see also [54]).

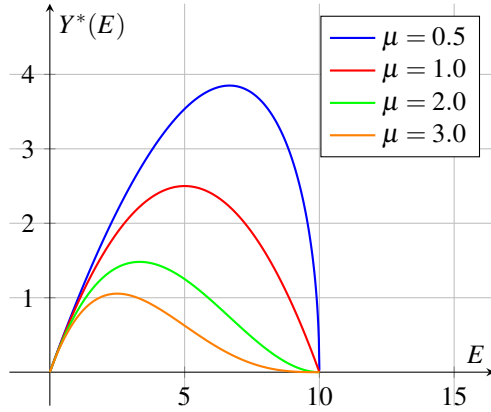


FIGURE 2. Function $Y^*(E)$ for different values of μ

206 **Example 3.** Let us consider the Gompertz equation with harvesting, which is used to de-
 207 scribe growth that slows down in a logarithmic manner (see [54]). It is often applied in
 208 tumor biology and demography. The differential equation is:

$$\frac{dx}{dt} = rx \ln \left(\frac{K}{x}\right) - Ex, \quad (3.9)$$

209 where r is the growth rate, K the carrying capacity, and E the fishing effort. This model
 210 captures rapid initial growth followed by a gradual slowdown as the population approaches
 211 the carrying capacity K . It is particularly useful for modeling systems in which growth
 212 decelerates over time, such as tumor growth or population dynamics.

213 The Gompertz growth equation (3.9) with constant harvesting has two equilibria: $x = 0$
 214 and $x^*(E) = Ke^{-\frac{E}{r}}$, which is positive for all values of E . At this equilibrium, the harvesting
 215 rate is:

$$Y^*(E) = Ex^*(E) = KEe^{-\frac{E}{r}}. \quad (3.10)$$

216 The derivative of the yield $Y^*(E)$ with respect to the fishing effort E is given by:

$$Y'(E) = K \cdot e^{-\frac{E}{r}} \left(1 - \frac{E}{r}\right)$$

217 Thus, the yield having a maximum for $E_{MSY}^* = r$ corresponding to the MSY. The corre-
 218 sponding value of the stable non-trivial positive equilibrium x^* reads as follows:

$$x_{MSY}^* := x^*(E_{MSY}^*) = \frac{K}{e}. \quad (3.11)$$

219 And the corresponding yield Y_{MSY}^* is given by the following expression:

$$Y_{MSY}^* = E_{MSY}^* x_{MSY}^* = \frac{rK}{e}. \quad (3.12)$$

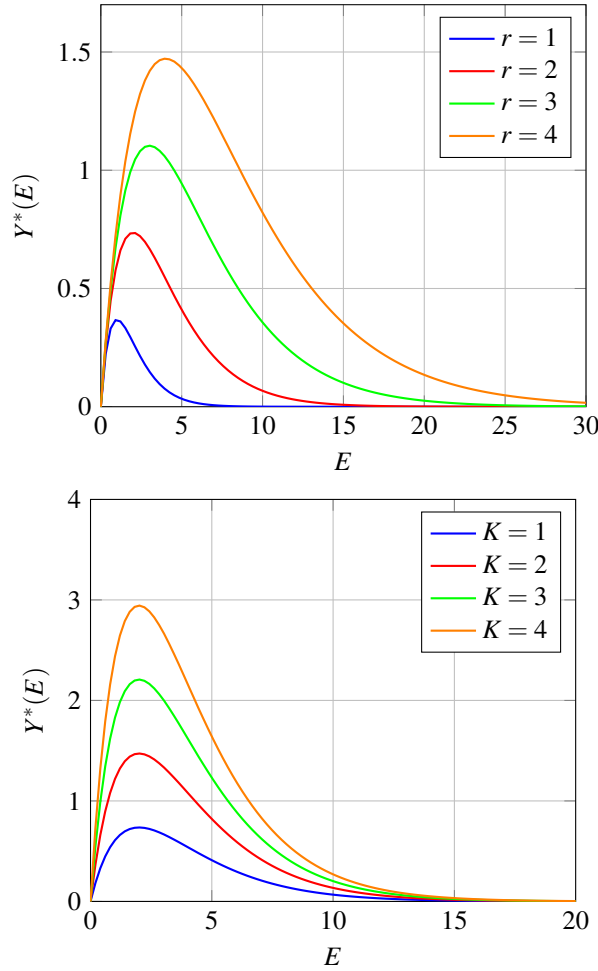


FIGURE 3. The function $Y^*(E) = EK e^{-\frac{E}{r}}$ for some values of r and K .

220 4. **Multi-patch case.** Let us consider the growth of a single species that can disperse
 221 among n patches, described by:

$$\frac{dx_i}{dt} = x_i \varphi_i(x_i) - E_i x_i + \varepsilon \sum_{j=1, j \neq i}^n (\gamma_{ij} h_j(x_j) - \gamma_{ji} h_i(x_i)), \quad i = 1, \dots, n, \quad (4.1)$$

222 where E_i are the fishing efforts. The terms $E_i x_i$ represent the Schaefer catch on patch i (see
 223 [56]), x_i denotes the population density of the species in the i -th patch, and $\varphi_i(x_i)$ is the
 224 specific growth rate of the population in the i -th patch. Since the specific growth rate may
 225 depend on the environment of each patch, the function $\varphi_i(x_i)$ is assumed to differ between
 226 patches.

227 The second term on the right-hand side of equation (4.1) describes the diffusion effect
 228 between patches, where ε is the migration rate, and $\gamma_{ij} \geq 0$ for all $i \neq j$ represents the
 229 asymmetric migration rate, describing the flow of individuals from patch j to patch i . The
 230 function $h_i(x_i)$ denotes the rate of dispersal out of the i -th habitat. These rates may, for
 231 example, depend on the distance between patches.

232 We list the following hypotheses, the first two of which are standard in single-species
233 models (see [35, 58]):

234 H1. All solutions of the initial value problem (4.1) exist, are unique and are continuable
235 for all positive time.

236 H2. $\varphi_i(0) > 0$, $\frac{d\varphi_i}{dx_i}(x_i) < 0$, there exist $K_i > 0$ such that $\varphi_i(K_i) = 0$ and $x_i\varphi_i(x_i) \rightarrow -\infty$ as
237 $x_i \rightarrow +\infty$ for all $i = 1, \dots, n$.

238 H3. $h_i(0) = 0$, $v_i \geq h'_i(x_i) \geq h'_i(0) > 0$ for all $i = 1, \dots, n$.

239 H4. The matrix $\Gamma := (\gamma_{ij})$ where

$$\gamma_{ii} = - \sum_{j=1, j \neq i}^n \gamma_{ji} \quad (4.2)$$

240 is irreducible.

241 In Hypothesis H2, K_i denotes the carrying capacity of the i -th patch. All patches are con-
242 sidered source patches since $\varphi_i(0) > 0$ for all i .

243 Hypothesis H3 states that the rate of dispersal out of the i -th patch is density-dependent
244 and increases with the population size in that patch. The requirement is mainly technical,
245 and v_i represents an upper bound on the growth rate of $h_i(x_i)$.

246 In Hypothesis H4, the irreducibility of the matrix Γ implies that the set of patches cannot
247 be partitioned into two non-empty disjoint subsets I and J such that there is no migration
248 between a patch in I and a patch in J . That is, the irreducibility of Γ ensures that every
249 patch in system (4.1) is connected via migration, meaning the species can reach any patch
250 i from any other patch j through a sequence of migrations.

251 In the two-patch case, the matrix Γ is irreducible if and only if both $\gamma_{12} > 0$ and $\gamma_{21} > 0$.

252 The functions $\varphi_i(x_i)$ and $h_i(x_i)$ play a crucial role in determining the dynamics of the
253 system. Below are some examples that satisfy Hypotheses H2 and H3, respectively.

- 254 • Logistic Growth: $\varphi_i(x_i) = r_i \left(1 - \frac{x_i}{K_i}\right)$, where $r_i > 0$ is the intrinsic growth rate and
255 $K_i > 0$ is the carrying capacity. This function satisfies H2 because: $\varphi_i(0) = r_i >$
256 0 , $\frac{d\varphi_i}{dx_i}(x_i) = -\frac{r_i}{K_i} < 0$, $\varphi_i(K_i) = 0$, and $x_i\varphi_i(x_i) \rightarrow -\infty$ as $x_i \rightarrow +\infty$.
- 257 • Linear Migration: $h_i(x_i) = m_i x_i$, where $m_i > 0$ is the migration rate coefficient. This
258 function satisfies H3 because: $h_i(0) = 0$ and $h'_i(x_i) = m_i > 0$.
- 259 • Saturating Migration (Michaelis-Menten Type): $h_i(x_i) = \frac{m_i x_i}{a_i + x_i}$, where $a_i > 0$ is the
260 half-saturation constant. This function satisfies H3 because: $h_i(0) = 0$ and $h'_i(x_i) =$
261 $\frac{m_i a_i}{(a_i + x_i)^2} > 0$.

4.1. **The total yield at MSY of connected and isolated fishing patches.** Assume that
 $E_i \leq \varphi_i(0)$ for all i , then according to [27], the model (4.1) has a unique positive equilibrium
point in the positive cone $\mathbb{R}_+^n \setminus \{0\}$. In all of this work, the positive equilibrium of the
system (4.1) is denoted by

$$\mathbb{E}_n^*(\varepsilon; E_1, \dots, E_n) = (x_1^*(\varepsilon; E_1, \dots, E_n), \dots, x_n^*(\varepsilon; E_1, \dots, E_n)),$$

262 which depends on migration rate ε and fishing efforts of all patches.

263 The components $x_i^*(\varepsilon; E_1, \dots, E_n)$, $i = 1, \dots, n$ of the equilibrium \mathbb{E}_n^* satisfied to the fol-
264 lowing equations:

$$\begin{aligned} x_i^*(\varepsilon; E_1, \dots, E_n) \varphi_i(x_i^*(\varepsilon; E_1, \dots, E_n)) - E_i x_i^*(\varepsilon; E_1, \dots, E_n) \\ + \varepsilon \sum_{j=1}^n \gamma_{ij} x_j^*(\varepsilon; E_1, \dots, E_n) = 0 \quad i = 1, \dots, n. \end{aligned} \quad (4.3)$$

265 The yield Y_i^* is given by

$$Y_i^*(\varepsilon; E_1, \dots, E_n) = E_i x_i^*(\varepsilon; E_1, \dots, E_n) = x_i^*(\varepsilon; E_1, \dots, E_n) \varphi_i(x_i^*(\varepsilon; E_1, \dots, E_n)) \\ + \varepsilon \sum_{j=1}^n \gamma_{ij} x_i^*(\varepsilon; E_1, \dots, E_n) \quad i = 1, \dots, n.$$

266 The sum of Y_i^* for $i = 1, \dots, n$ gives the total Yield Y_T^* of n connected patches:

$$Y_T^*(\varepsilon; E_1, \dots, E_n) = \sum_{i=1}^n x_i^*(\varepsilon; E_1, \dots, E_n) \varphi_i(x_i^*(\varepsilon; E_1, \dots, E_n)).$$

267 Hence,

$$Y_{MSY,T}^*(\varepsilon) = \max_{(E_1, \dots, E_n)} \sum_{i=1}^n x_i^*(\varepsilon; E_1, \dots, E_n) \varphi_i(x_i^*(\varepsilon; E_1, \dots, E_n)). \quad (4.4)$$

268 For $\varepsilon = 0$, the sum of MSY of each isolated patches take the following form:

$$Y_{MSY,T}^*(0) = \max_{(E_1, \dots, E_n)} \sum_{i=1}^n x_i^*(0; E_i) \varphi_i(x_i^*(0; E_i)) \\ = \sum_{i=1}^n \max_{0 \leq E_i \leq \varphi_i(0)} x_i^*(0; E_i) \varphi_i(x_i^*(0; E_i)) \\ = \sum_{i=1}^n \max_{0 \leq x_i \leq K_i} x_i \varphi_i(x_i).$$

269 **4.2. Comparison of MSY catches between connected fishing patches via migration**
 270 **and isolated fishing patches.** Now, we are going to compare at MSY the total yield for
 271 the system (4.1), $Y_{MSY,T}^*(\varepsilon)$, given by the formula (4.4), with the sum of yields for n isolated
 272 patches, $Y_{MSY,T}^*(0)$, as the migration rate ε varies from 0 to ∞ .

273 Thus, we generalize and extend the results of Auger et al. [4] for the two-patch model
 274 with harvesting to the multi-patch model with harvesting (4.1). We have the following
 275 result:

Theorem 4.1. Consider the MSY (4.4) of the total Yield, then, for all $\varepsilon \geq 0$, we have:

$$Y_{MSY,T}^*(\varepsilon) \leq Y_{MSY,T}^*(0).$$

276 *Proof.* We have for all $\varepsilon \geq 0$:

$$Y_{MSY,T}^*(\varepsilon) = \max_{(E_1, \dots, E_n)} \sum_{i=1}^n x_i^*(\varepsilon; E_1, \dots, E_n) \varphi_i(x_i^*(\varepsilon; E_1, \dots, E_n)), \\ \leq \max_{(E_1, \dots, E_n)} \sum_{i=1}^n \max_{x_i} x_i \varphi_i(x_i), \\ \leq Y_{MSY,T}^*(0).$$

277

□

278 As a first corollary of the previous Theorem, we have:

Corollary 1. Assume that: $\varphi_i(x_i) = r_i \left(1 - \frac{x_i}{K_i}\right)$ for all i . Consider the MSY (4.4) of the total Yield, then, for all $\varepsilon \geq 0$, we have:

$$Y_{MSY,T}^*(\varepsilon) \leq Y_{MSY,T}^*(0) = \sum_{i=1}^n \frac{1}{4} r_i K_i.$$

Proof. The function φ_i satisfies to hypothesis H2. The derivative of $x_i^* \varphi_i(x_i^*)$ with respect to x_i^* gives:

$$\frac{d(x_i^* \varphi_i)}{dx_i^*}(x_i^*) = -r_i \left[-1 + 2 \left(\frac{x_i^*}{K_i} \right) \right].$$

279 Therefore, $\frac{d(x_i^* \varphi_i)}{dx_i^*}(x_i^*) = 0$ if and only if $x_i^* = \frac{K_i}{2}$. In that case, the maximum of $x_i^* \varphi_i$ is equal
280 to $1/4r_i K_i$. Hence, the completes proof of corollary. \square

281 As a second corollary of the previous Theorem, we have:

Corollary 2. Assume that: $\varphi_i(x_i) = r_i \left[1 - \left(\frac{x_i}{K_i} \right)^{\mu_i} \right]$ for all i . Consider the MSY (4.4) of the total Yield, then, for all $\varepsilon \geq 0$ and for all $\mu > 0$, we have:

$$Y_{MSY,T}^*(\varepsilon) \leq Y_{MSY,T}^*(0) = \sum_{i=1}^n \mu_i \left(\frac{1}{\mu_i + 1} \right)^{\mu_i^{-1} + 1} r_i K_i.$$

Proof. The function φ_i satisfies to hypothesis H2. The derivative of $x_i^* \varphi_i$ with respect to x_i^* gives:

$$\frac{d(x_i^* \varphi_i)}{dx_i^*}(x_i^*) = -r_i \left[-1 + \left(\frac{x_i^*}{K_i} \right)^{\mu_i} + \left(\frac{x_i^*}{K_i} \right)^{\mu_i} \mu_i \right].$$

282 Therefore, $\frac{d(x_i^* \varphi_i)}{dx_i^*}(x_i^*) = 0$ if and only if $x_i^* = \frac{1}{(\mu_i + 1)^{\frac{1}{\mu_i}}} K_i$. In that case, the maximum of $x_i^* \varphi_i$

283 is equal to $\frac{\mu_i}{\mu_i + 1} \left(\frac{1}{\mu_i + 1} \right)^{\mu_i^{-1}} r_i K_i$. Hence, the completes proof of corollary. \square

284 As a third corollary of the previous Theorem, we have:

Corollary 3. Assume that: $\varphi_i(x_i) = r_i \ln \left(\frac{K_i}{x_i} \right)$ for all i . Consider the MSY (4.4) of the total Yield, then, for all $\varepsilon \geq 0$, we have:

$$Y_{MSY,T}^*(\varepsilon) \leq Y_{MSY,T}^*(0) = \sum_{i=1}^n \frac{1}{e} r_i K_i.$$

Proof. The function φ_i satisfies to hypothesis H2. The derivative of $x_i^* \varphi_i$ with respect to x_i^* gives:

$$\frac{d(x_i^* \varphi_i)}{dx_i^*}(x_i^*) = r_i \ln \left(\frac{K_i}{x_i^*} \right) - r_i$$

285 Therefore, $\frac{d(x_i^* \varphi_i)}{dx_i^*}(x_i^*) = 0$ if $x_i^* = K_i/e$. In that case, the maximum of $x_i^* \varphi_i$ is equal to $\frac{1}{e} r_i K_i$.

286 Hence, the completes proof of corollary. \square

287 **4.3. Variation of the total yield at MSY as function of migration.** The following theo-
288 rem establishes a fundamental quantitative relationship between habitat connectivity and
289 sustainable fishery productivity in multi-patch systems. It reveals a universal ecological
290 constraint: in any network of interconnected habitats where populations follow realistic
291 growth dynamics, intensification of migratory exchanges necessarily reduces the maxi-
292 mum sustainable yield (MSY) of the entire system. Mathematically, we have the following
293 result:

294 **Theorem 4.2.** Assume that: $\varphi_i(x_i) + x_i \varphi_i'(x_i) < 0$ for all i . Consider the multi-patch system
295 (4.1) under assumptions (H1)-(H4), then, the total maximum sustainable yield $Y_{MSY,T}^*(\varepsilon)$ is
296 a decreasing function of the migration rate ε , i.e.,

$$\frac{dY_{MSY,T}^*}{d\varepsilon}(\varepsilon) \leq 0 \quad \text{for all } \varepsilon \geq 0.$$

297 *Proof.* At equilibrium ($dx_i/dt = 0$):

$$x_i^* \varphi_i(x_i^*) - E_i x_i^* + \varepsilon \sum_{j=1}^n \gamma_{ij} h_j(x_j^*) = 0 \quad (1) \quad (4.5)$$

298 The total yield is:

$$Y_T^*(\varepsilon) = \sum_{i=1}^n E_i x_i^*(\varepsilon) \quad (4.6)$$

299 Differentiate (4.5) with respect to ε :

$$[\varphi_i(x_i^*) + x_i^* \varphi_i'(x_i^*) - E_i] \frac{dx_i^*}{d\varepsilon} + \sum_{j=1}^n \gamma_{ij} h_j(x_j^*) + \varepsilon \sum_{j=1}^n \gamma_{ij} h_j'(x_j^*) \frac{dx_j^*}{d\varepsilon} = 0 \quad (4.7)$$

300 Denote $\varphi_i(x_i^*) + x_i^* \varphi_i'(x_i^*) := A_i(x_i^*)$. Let $D_i := A_i(x_i^*) - E_i$. The matrix form is:

$$\mathbf{D} \frac{dx^*}{d\varepsilon} + \Gamma h(x^*) + \varepsilon \Gamma \mathbf{H} \frac{dx^*}{d\varepsilon} = 0 \quad (4.8)$$

301 where: $x^* = (x_1^*, \dots, x_n^*)$, $\mathbf{D} = \text{diag}(D_1, \dots, D_n)$, $h(x_1^*) = (h_1(x_1^*), \dots, h_n(x_n^*))^T$
 302 and $\mathbf{H} = \text{diag}(h_1'(x_1^*), \dots, h_n'(x_n^*))$. The previous equation implies that:

$$[\mathbf{D} + \varepsilon \Gamma \mathbf{H}] \frac{dx^*}{d\varepsilon} = -\Gamma h(x^*) \quad (4.9)$$

303 Under assumptions (H1)-(H4), the matrix $\mathbf{M} := \mathbf{D} + \varepsilon \Gamma \mathbf{H}$ is invertible for $\varepsilon \geq 0$. Indeed,
 304 From the assumption $\varphi_i + x_i \varphi_i' < 0$ and harvesting $E_i \geq 0$, we have:

$$D_i = \varphi_i(x_i^*) + x_i^* \varphi_i'(x_i^*) - E_i < 0 \quad \text{for all } i.$$

305 For $\varepsilon > 0$, consider the row sums of \mathbf{M} :

$$|M_{ii}| - \sum_{j \neq i} |M_{ij}| = |D_i + \varepsilon \Gamma_{ii} h_i'(x_i^*)| - \varepsilon \sum_{j \neq i} |\Gamma_{ij} h_j'(x_j^*)|$$

306 Since $\Gamma_{ii} = -\sum_{j \neq i} \gamma_{ji} < 0$ and $\Gamma_{ij} = \gamma_{ij} \geq 0$ ($i \neq j$), and $h_j' > 0$ (from H3):

$$|M_{ii}| - \sum_{j \neq i} |M_{ij}| = -D_i - \varepsilon \Gamma_{ii} h_i'(x_i^*) - \varepsilon \sum_{j \neq i} \Gamma_{ij} h_j'(x_j^*) = -D_i + \varepsilon \left(\sum_{j \neq i} \gamma_{ji} h_i'(x_i^*) - \sum_{j \neq i} \gamma_{ij} h_j'(x_j^*) \right)$$

307 From (H4), Γ is irreducible. By the Levy-Desplanques theorem, a strictly diagonally dom-
 308 inant matrix with non-positive diagonal entries and non-negative off-diagonal entries is
 309 non-singular. Here: Diagonal entries $M_{ii} = D_i + \varepsilon \Gamma_{ii} h_i'(x_i^*) < 0$ and Off-diagonal entries
 310 $M_{ij} = \varepsilon \Gamma_{ij} h_j'(x_j^*) \geq 0$ for $i \neq j$. The matrix \mathbf{M} can be written as:

$$\mathbf{M} = \mathbf{D} + \varepsilon \Gamma \mathbf{H} = \mathbf{D} - \varepsilon \tilde{\Gamma}$$

311 where $\tilde{\Gamma}$ is a Metzler matrix (non-negative off-diagonal). Since $\mathbf{D} < 0$ (negative definite
 312 diagonal) and $\tilde{\Gamma} \geq 0$, the eigenvalues of \mathbf{M} satisfy:

$$\text{Re}(\lambda(\mathbf{M})) \leq \max_i D_i < 0$$

313 Thus, \mathbf{M} cannot have a zero eigenvalue. Therefore, $\mathbf{D} + \varepsilon \Gamma \mathbf{H}$ is invertible for all $\varepsilon \geq 0$.
 314 Hence,

$$\frac{dx^*}{d\varepsilon} = -[\mathbf{D} + \varepsilon \Gamma \mathbf{H}]^{-1} \Gamma h(x^*) \quad (4.10)$$

315 Yield Derivative is given by:

$$\frac{dY_T^*}{d\varepsilon} = E^\top \frac{dx^*}{d\varepsilon} = -E^\top [\mathbf{D} + \varepsilon \Gamma \mathbf{H}]^{-1} \Gamma h(x^*) \quad (4.11)$$

316 We have, For $\varepsilon \geq 0$: Γ is Metzler with negative diagonal (H4), the vector $h(x^*) \geq 0$
 317 component-wise (H3) and $[\mathbf{D} + \varepsilon\Gamma\mathbf{H}]^{-1}$ is non-positive. Thus:

$$\frac{dY_T^*}{d\varepsilon} = - \underbrace{E^\top}_{\geq 0} \underbrace{[\mathbf{D} + \varepsilon\Gamma\mathbf{H}]^{-1}}_{\leq 0} \underbrace{\Gamma}_{\leq 0} \underbrace{h(x^*)}_{\geq 0} \leq 0 \quad (4.12)$$

318

□

319 **Example 4.** For identical patches with symmetric migration, the equilibrium equations
 320 are:

$$\begin{cases} rx_1^* \left(1 - \frac{x_1^*}{K}\right) - Ex_1^* + \varepsilon\gamma(x_2^* - x_1^*) = 0 \\ rx_2^* \left(1 - \frac{x_2^*}{K}\right) - Ex_2^* + \varepsilon\gamma(x_1^* - x_2^*) = 0 \end{cases} \quad (4.13)$$

321 Rewrite (4.13) as:

$$\begin{pmatrix} r(1 - \frac{2x_1^*}{K}) - E - \varepsilon\gamma & \varepsilon\gamma \\ \varepsilon\gamma & r(1 - \frac{2x_2^*}{K}) - E - \varepsilon\gamma \end{pmatrix} \begin{pmatrix} dx_1^*/d\varepsilon \\ dx_2^*/d\varepsilon \end{pmatrix} = -\gamma \begin{pmatrix} x_2^* - x_1^* \\ x_1^* - x_2^* \end{pmatrix} \quad (4.14)$$

322 The total yield is $Y_T^* = E(x_1^* + x_2^*)$. Its derivative:

$$\frac{dY_T^*}{d\varepsilon} = E \left(\frac{dx_1^*}{d\varepsilon} + \frac{dx_2^*}{d\varepsilon} \right) = -E\gamma(1 \quad 1) \mathbf{J}^{-1} \begin{pmatrix} x_2^* - x_1^* \\ x_1^* - x_2^* \end{pmatrix} \quad (4.15)$$

323 where \mathbf{J} is the Jacobian matrix evaluated at equilibrium.

324 At MSY, $E = r/2$ and $x_1^* = x_2^* = K/2$. The Jacobian becomes:

$$\mathbf{J} = \begin{pmatrix} -r - \varepsilon\gamma & \varepsilon\gamma \\ \varepsilon\gamma & -r - \varepsilon\gamma \end{pmatrix} \quad (4.16)$$

325 with inverse:

$$\mathbf{J}^{-1} = \frac{1}{(r + \varepsilon\gamma)^2 - (\varepsilon\gamma)^2} \begin{pmatrix} -r - \varepsilon\gamma & -\varepsilon\gamma \\ -\varepsilon\gamma & -r - \varepsilon\gamma \end{pmatrix} \quad (4.17)$$

326 Substituting into (4.15):

$$\frac{dY_T^*}{d\varepsilon} = -\frac{r}{2}\gamma(1 \quad 1) \frac{1}{r(r + 2\varepsilon\gamma)} \begin{pmatrix} -r - \varepsilon\gamma & -\varepsilon\gamma \\ -\varepsilon\gamma & -r - \varepsilon\gamma \end{pmatrix} \begin{pmatrix} 0 \\ 0 \end{pmatrix} = -\frac{r^2K\gamma}{2(r + 2\varepsilon\gamma)^2} \quad (4.18)$$

327 Alternatively, starting from the symmetric solution:

$$x^* = \frac{K(r - E)}{r + 2\varepsilon\gamma} \quad (4.19)$$

328 Total yield at MSY ($E = r/2$):

$$Y_{MSY}^* = 2 \cdot \frac{r}{2} \cdot \frac{K(r - r/2)}{r + 2\varepsilon\gamma} = \frac{r^2K}{2(r + 2\varepsilon\gamma)} \quad (4.20)$$

329 Differentiating:

$$\frac{dY_{MSY}^*}{d\varepsilon} = -\frac{r^2K \cdot 2\gamma}{2(r + 2\varepsilon\gamma)^2} = -\frac{r^2K\gamma}{(r + 2\varepsilon\gamma)^2} \quad (4.21)$$

330 **5. Numerical simulations.** In this section, we will conduct some numerical simulations
 331 to further investigate the effect of different parameters of the model and interconnections
 332 on the Maximum Sustainable Yield in a heterogeneous environment and demonstrate our
 333 theoretical findings of Theorems 4.1 and 4.2. Note that, the parameter values used below
 334 are for illustrative purposes only and are not intended to be biologically realistic.

335 **5.1. Illustration the result of Theorem 4.1.**

336 **Example 5.** We consider the system of two patch with harvesting, i.e. (4.1) and we assume
 337 that the first patch follows a logistic law, while the second patch follows a Richards law.
 338 The model read as follow:

$$\begin{cases} \frac{dx_1}{dt} = 2x_1(1-x_1) - E_1x_1 + \varepsilon(x_2 - x_1), \\ \frac{dx_2}{dt} = 3x_2\left(1 - \left[\frac{x_2}{2}\right]^2\right) - E_2x_2 + \varepsilon(x_1 - x_2). \end{cases} \quad (5.1)$$

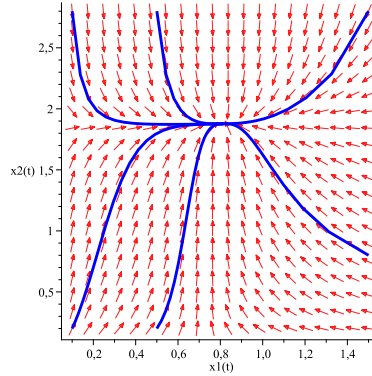


FIGURE 4. Trajectories of the Coupled System (5.1) with $E_1 = 0.5, E_2 = 0.3, \varepsilon = 0.1$

339

340 The sum of MSY of each isolated patches ($\varepsilon = 0$) is given by

$$Y_{MSY,T}^*(0) = \mu_1 \left(\frac{1}{\mu_1 + 1}\right)^{\mu_1^{-1}+1} r_1 K_1 + \mu_2 \left(\frac{1}{\mu_2 + 1}\right)^{\mu_2^{-1}+1} r_2 K_2 \simeq 2.809401076. \quad (5.2)$$

341 **Example 6.** We consider the system of two patch with harvesting, i.e. (4.1) and we assume
 342 that the both patches follows a Gompertz law. The model read as follow:

$$\begin{cases} \frac{dx_1}{dt} = 3x_1 \ln\left(\frac{1}{x_1}\right) - E_1x_1 + \varepsilon(2x_2 - x_1), \\ \frac{dx_2}{dt} = 2x_2 \ln\left(\frac{4}{x_2}\right) - E_2x_2 + \varepsilon(x_1 - 2x_2). \end{cases} \quad (5.3)$$

343

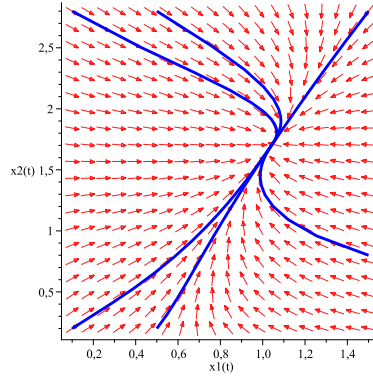


FIGURE 5. Trajectories of the Coupled System (5.3) with $E_1 = 1, E_2 = 1, \varepsilon = 0.5$

344 The sum of MSY of each isolated patches ($\varepsilon = 0$) is given by

$$Y_{MSY,T}^*(0) = 1/e(r_1K_1 + r_2K_2) \simeq 4.046673854. \quad (5.4)$$

345 We propose here to plot the total yield $Y_T^*(\varepsilon, E_1, E_2) = (Y_1^* + Y_2^*)(\varepsilon, E_1, E_2)$ with respect
 346 to the fishing efforts E_1 and E_2 and also these projections in the plan $E_1 = 0$ and $E_2 = 0$,
 347 for $\varepsilon = 0$ and for $\varepsilon \rightarrow \infty$.

In the table 1, we compute $Y_{MSY,T}^*(\varepsilon)$, $(\Delta Y_{MSY,T}^*)(\varepsilon)$ and $\% \Delta Y_{MSY,T}^*$. The Yield excess $\Delta Y_{MSY,T}^*$ is given by the following formula:

$$(\Delta Y_{MSY,T}^*)(\varepsilon) = Y_{MSY,T}^*(\varepsilon) - Y_{MSY,T}^*(0),$$

and the percentage of yield excess is define as:

$$(\% \Delta Y_{MSY,T}^*)(\varepsilon) = 100 \frac{(\Delta Y_{MSY,T}^*)(\varepsilon)}{Y_{MSY,T}^*(\varepsilon)}.$$

TABLE 1. Values of $Y_{MSY,T}$ and $\Delta Y_{MSY,T}$ obtained for the models (5.1) and (5.3) and for migration rate $\varepsilon = 0$ and ε close to ∞ .

Figures	ε	$Y_{MSY,T}^*(\varepsilon)$	$(\Delta Y_{MSY,T}^*)(\varepsilon)$	$\% \Delta Y_{MSY,T}^*$
Fig. 6	0	2.80	-0.00	00.00%
Fig. 7	∞	2.30	-0.50	21.73%
Fig. 8	0	4.04	-0.00	00.00%
Fig. 9	∞	2.68	-1.36	50.74%

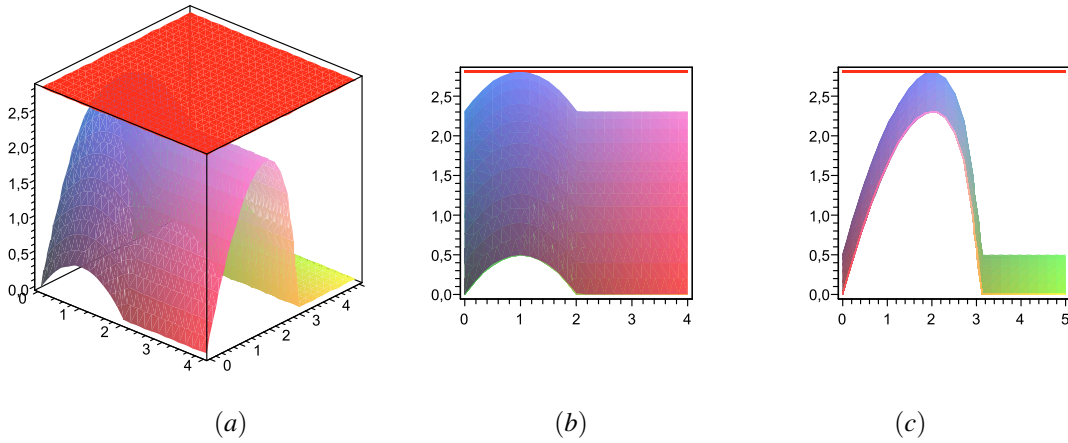


FIGURE 6. Case a: The total yield $Y_T^*(0, E_1, E_2) = (Y_1^* + Y_2^*)(0, E_1, E_2)$ with respect to the fishing effort $E_1 \in [0, 4]$ and $E_2 \in [0, 5]$ which is shown in blue, and the total yield $Y_T^*(0, E_1, E_2) = 2.80$ is shown in red for the model 5.1 and the migration rate ε equal to 0. Case b (resp. c): the projection of the total yields $Y_T^*(0, E_1, E_2)$ and $Y_T^*(0, E_1, E_2) \simeq 2.80$ in

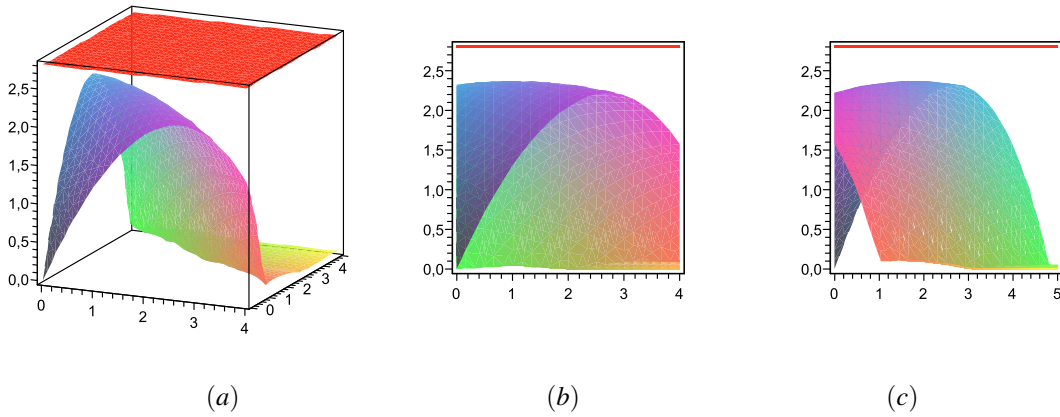


FIGURE 7. Case a: The total yield $Y_T^*(\infty, E_1, E_2) = (Y_1^* + Y_2^*)(\infty, E_1, E_2)$ with respect to the fishing effort $E_1 \in [0, 4]$ and $E_2 \in [0, 5]$ which is shown in blue, and the total yield $Y_T^*(0, E_1, E_2) = 2.80$ is shown in red for the model 5.1 and the migration rate $\varepsilon \rightarrow \infty$. Case b (resp. c): the projection of the total yields $Y_T^*(\infty, E_1, E_2)$ and $Y_T^*(0, E_1, E_2) \simeq 2.80$ in the plan $E_2 = 0$ (resp. $E_1 = 0$).

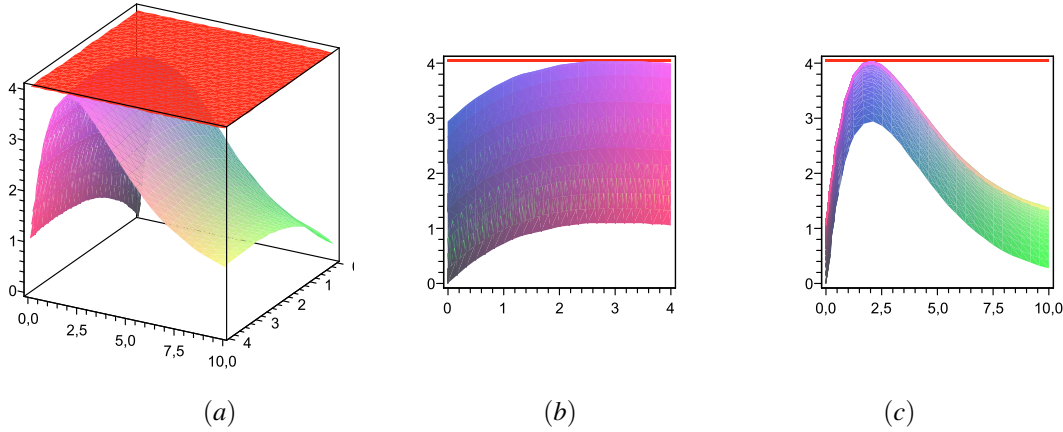


FIGURE 8. Case a: The total yield $Y_T^*(0, E_1, E_2) = (Y_1^* + Y_2^*)(0, E_1, E_2)$ with respect to the fishing effort $E_1 \in [0, 4]$ and $E_2 \in [0, 10]$ which is shown in blue, and the total yield $Y_T^*(0, E_1, E_2) = 4.04$ is shown in red for the model 5.3 and the migration rate ε equal to 0. Case b (resp. c): the projection of the total yields $Y_T^*(0, E_1, E_2)$ and $Y_T^*(0, E_1, E_2) \simeq 4.04$ in the plan $E_1 = 0$ (resp. $E_2 = 0$).

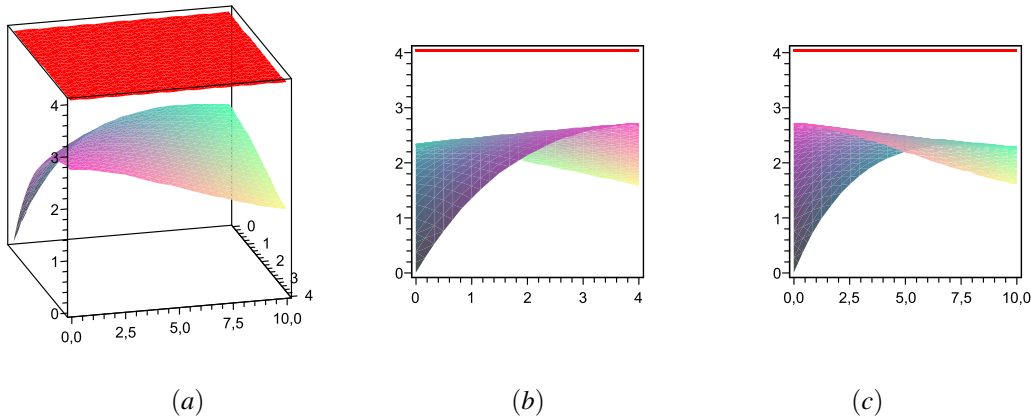


FIGURE 9. Case a: The total yield $Y_T^*(\infty, E_1, E_2) = (Y_1^* + Y_2^*)(\infty, E_1, E_2)$ with respect to the fishing effort $E_1 \in [0, 4]$ and $E_2 \in [0, 10]$ which is shown in blue, and the total yield $Y_T^*(0, E_1, E_2) = 4.04$ is shown in red for the model 5.3 and the migration rate $\varepsilon \rightarrow \infty$. Case b (resp. c): the projection of the total yields $Y_T^*(0, E_1, E_2)$ and $Y_T^*(0, E_1, E_2) \simeq 4.04$ in the plan $E_2 = 0$ (resp. $E_1 = 0$).

348 **5.2. Illustration the result of Theorem 4.2.** The four curves in Figures 12 and 15 present
 349 a comparative analysis of how migration rates (ε) affect the total yield at MSY ($Y_{MSY,T}^*$)
 350 across different population models. Each figure illustrates distinct biological growth dy-
 351 namics: (1) Logistic-Richards with $Y_{MSY,T}^*(0) = 2.809$, (2) Gompertz-Gompertz with $Y_{MSY,T}^*(0) =$
 352 4.047, (3) Logistic-Logistic with $Y_{MSY,T}^*(0) = 3.500$, and (4) Richards-Richards with $Y_{MSY,T}^*(0) =$
 353 3.200.

354 All models demonstrate an exponential decay in total yield at MSY as migration rate ε
 355 increases, with two key observations:

356 First, the Gompertz model shows the steepest decline due to its logarithmic growth
357 constraint, with total yields at MSY dropping by approximately 34% at $\varepsilon = 5$.

358 Second, models with asymmetric parameters (Richards) exhibit a slower decay (only an
359 18% reduction at $\varepsilon = 5$), suggesting greater structural resilience to migration effects.

360 This analysis highlights a fundamental trade-off in resource management: while mi-
361 gration enhances ecological connectivity, it systematically reduces short-term profitability,
362 with the severity depending on the population's growth characteristics. The results suggest
363 that optimal fishery management should account for both species-specific growth dynamics
364 and patch connectivity levels when setting harvesting policies. In particular:

- 365 • Fisheries dominated by Gompertz-type growth require more conservative manage-
366 ment at high migration rates.
- 367 • Richards-type systems may tolerate higher connectivity while maintaining yields.

368 **6. Conclusion and Perspectives.** In this work, we investigated the influence of gener-
369 alized growth functions on the determination of the Maximum Sustainable Yield (MSY)
370 in both single-species and spatially structured multi-patch fishery models. Starting with
371 a general formulation of population growth, we analyzed how different functional forms
372 specifically the logistic, Richards, and Gompertz models affect the equilibrium biomass
373 under harvesting and derived explicit expressions for MSY in each case. These results
374 reveal that the intrinsic shape of the growth function directly influences both the optimal
375 biomass level and the corresponding harvesting effort, thus affecting management recom-
376 mendations. Notably, the Richards model with its adjustable shape parameter offers a
377 flexible framework that encompasses the logistic model as a special case and allows higher
378 yields under certain conditions.

379 In the multi-patch setting, we extended the analysis to systems with spatial dispersal be-
380 tween patches and demonstrated, both analytically and numerically, that the total MSY of
381 a connected system is always less than or equal to the sum of MSYs obtained when patches
382 are managed in isolation. This result holds under general biological assumptions and is
383 shown to be robust across different growth models and migration patterns. Moreover, we
384 proved that the total yield at MSY decreases monotonically with increasing migration rate,
385 highlighting a counterintuitive trade-off: while dispersal may enhance population persis-
386 tence, it simultaneously reduces the maximum yield that can be sustainably harvested from
387 the entire system. These findings provide a rigorous theoretical foundation for understand-
388 ing how spatial connectivity and intrinsic growth dynamics interact to shape harvesting
389 potential in ecological systems.

390 To further improve the ecological relevance and practical utility of the proposed model-
391 ing approach, future work could explore several valuable extensions. A key direction is
392 the incorporation of predator-prey dynamics, especially in situations where the predator is
393 also subject to harvesting. This would provide a richer representation of trophic interac-
394 tions and their implications for the sustainable management of ecosystems. Additionally,
395 introducing stochastic components—such as environmental fluctuations or demographic
396 randomness—would allow for the analysis of MSY under uncertain conditions, thereby
397 enhancing the robustness and reliability of management recommendations.

398 REFERENCES

- 399 [1] Allen, L. J. S.: Persistence and extinction in Lotka-Volterra reaction-diffusion equations. *Math. Biosci.* 65,
400 1-12 (1983)
- 401 [2] Allen, L. J. S.: Persistence and extinction in single-species reaction-diffusion models. *Bull. Math. Biol.* 45,
402 209-227 (1983)

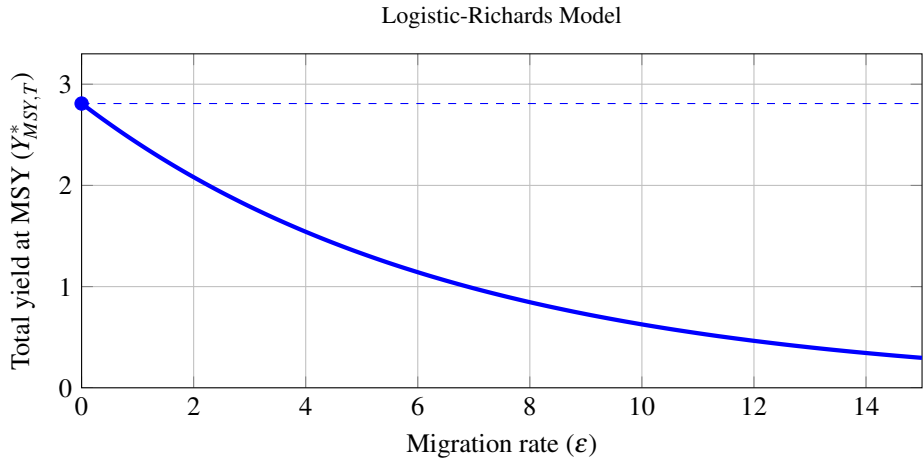


FIGURE 10. Parameters: $r_1 = 2, K_1 = 1, \mu = 2$
 Initial profit: $Y_{MSY,T}^*(0) = 2.809$

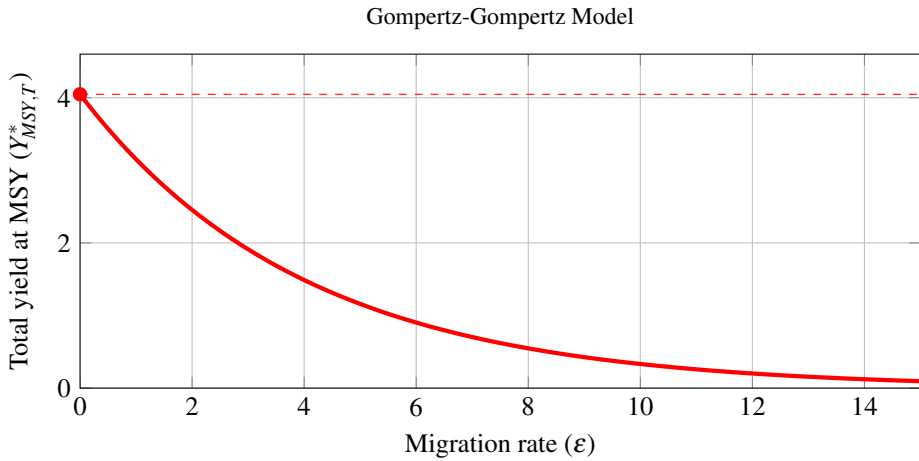


FIGURE 11. Parameters: $r_1 = 3, K_1 = 1, r_2 = 2, K_2 = 4$
 Initial profit: $Y_{MSY,T}^*(0) = 4.047$

FIGURE 12. Impact of migration rate on total yield at MSY, $Y_{MSY,T}^*$, for different population models for two patches case.

403 [3] Allen, L. J. S.: Persistence, extinction, and critical patch number for island populations. *J. Math. Biol.* 24,
 404 617-625 (1987)
 405 [4] P. Auger, B. Kooi, A. Moussaoui, Increase of maximum sustainable yield for fishery in two patches with fast
 406 migration, *Ecological Modelling* 467 (2022) 109898 [https://doi.org/10.1016/j.ecolmodel.2022.](https://doi.org/10.1016/j.ecolmodel.2022.109898)
 407 [109898](https://doi.org/10.1016/j.ecolmodel.2022.109898)
 408 [5] P. Auger, C.Lett, A. Moussaoui, S. Pioch, Optimal number of sites in artificial pelagic multisite fisheries.
 409 *Aquatic Living Resources*, 13 (2000), 253-257.
 410 [6] P. Auger, T. Nguyen-Huu and D. Nguyen-Ngoc, On the impossibility of increasing the MSY in a multisite
 411 Schaefer fishing model, *MBE*, 22(2): 415–430, 2025.

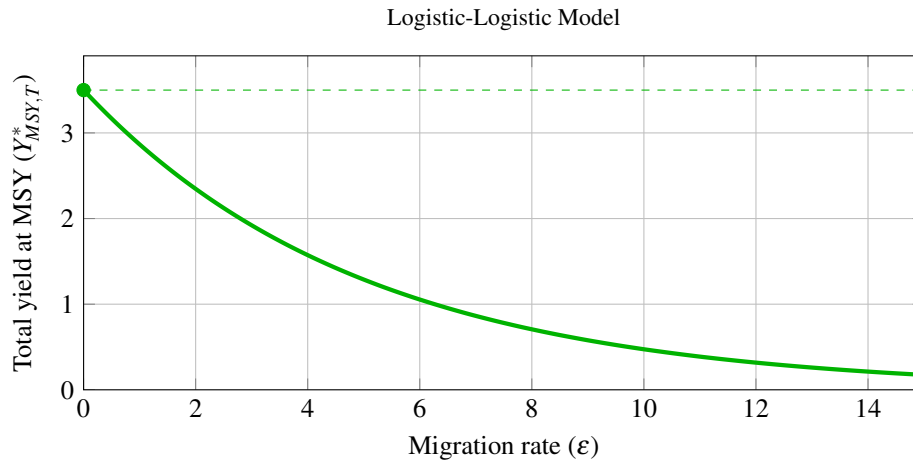


FIGURE 13. Parameters: $r_1 = 2.5$, $K_1 = 1.4$, $r_2 = 2$, $K_2 = 1.8$
Initial profit: $Y_{MSY,T}^*(0) = 3.500$.

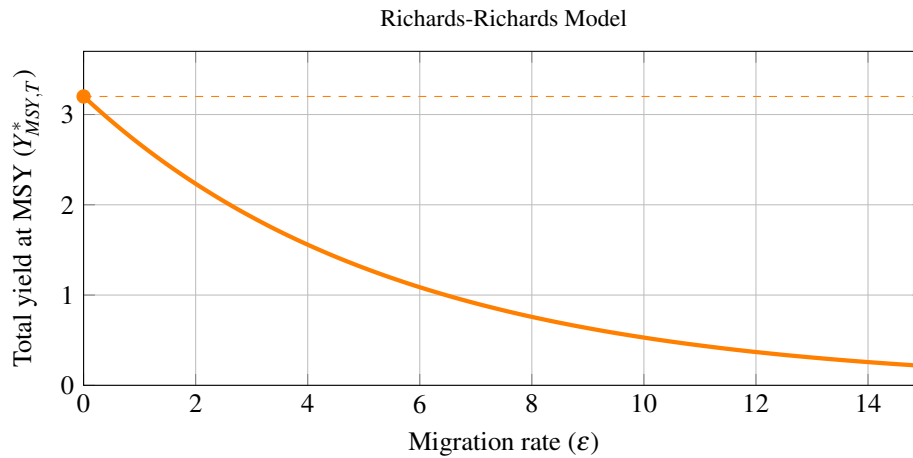


FIGURE 14. Parameters: $r_1 = 3$, $K_1 = 1.2$, $\mu_1 = 1.5$, $r_2 = 2.5$, $K_2 = 1.5$,
 $\mu_2 = 2$ Initial profit: $Y_{MSY,T}^*(0) = 3.200$

FIGURE 15. Impact of migration rate on total yield at MSY, $Y_{MSY,T}^*$, for different population models for two patches case.

- 412 [7] R. Arditi, C. Lobry and T. Sari, In dispersal always beneficial to carrying capacity? New insights from the
413 multi-patch logistic equation, *Theoretical Population Biology*, 106 (2015), 45-59. [http://doi:10.1016/](http://doi:10.1016/j.tpb.2015.10.001)
414 [j.tpb.2015.10.001](http://doi:10.1016/j.tpb.2015.10.001).
- 415 [8] R. Arditi, C. Lobry and T. Sari, Asymmetric dispersal in the multi-patch logistic equation, *Theoretical*
416 *Population Biology*, 120 (2018), 11-15. <http://doi:10.1016/j.tpb.2017.12.006>.
- 417 [9] J. Arino, N. Bajeux and S. Kirkland, Number of Source Patches Required for Population Persistence in a
418 Source-Sink Metapopulation with Explicit Movement, *Bulletin of Mathematical Biology* (2019) 81:1916-
419 1942. <https://doi.org/10.1007/s11538-019-00593-1>
- 420 [10] J. Arino, Diseases in metapopulations, in *Modeling and Dynamics of Infectious Diseases*, Z. Ma, Y. Zhou,
421 J. Wu (eds.), Series in Contemporary Applied Mathematics, World Scientific Press, Vol. 11 (2009), 64-122.

- 422 [11] M. Bensenane, A. Moussaoui, P. Auger, On the Optimal Size of Marine Reserves. *Acta Biotheoretica*, 61
423 (2013), 109-118.
- 424 [12] M. Benaim, C. Lobry, T. Sari, E. Strickler. When can a population spreading across sink habitats persist ?
425 2023. [hal-04099082](https://hal.science/hal-04099082)
- 426 [13] M. Benaim, C. Lobry, T. Sari and E. Strickler, Untangling the role of temporal and spatial variations in
427 persistence of populations. (2022) [arXiv:2111.12633](https://arxiv.org/abs/2111.12633).
- 428 [14] R. Bravo de la Parra, J. C. Poggiale, P. Auger The effect of connecting sites in the environment of a harvested
429 population. *Math. Model. Nat. Phenom.* 18 (2023), 4.
- 430 [15] C.W. Clark. *Mathematical Bioeconomics. The Optimal Management of Renewable Resources.* 2nd ed. John
431 Wiley and Sons, Inc., New York (1990).
- 432 [16] C. Cosner, J. C. Beier, R. S. Cantrell, D. Impoinvil, L. Kapitanski, M. D. Potts, A. Troyo, and S. Ruan, The
433 effects of human movement on the persistence of vector-borne diseases, *J. Theoret. Biol.*, 258 (2009), pp.
434 550-560.
- 435 [17] D. L. DeAngelis, C. C. Travis and W. M. Post, Persistence and stability of seed-dispersal species in
436 a patchy environment, *Theoretical Population Biology*, 16 (1979), 107-125. [http://dx.doi.org/10.](https://dx.doi.org/10.1016/0040-5809(79)90008-X)
437 [1016/0040-5809\(79\)90008-X](https://dx.doi.org/10.1016/0040-5809(79)90008-X).
- 438 [18] D. L. DeAngelis and B. Zhang, Effects of dispersal in a non-uniform environment on population dynamics
439 and competition: a patch model approach, *Discrete Contin. Dyn. Syst. Ser. B*, 19 (2014), 3087-3104. [http:](https://dx.doi.org/10.3934/dcdsb.2014.19.3087)
440 [//dx.doi.org/10.3934/dcdsb.2014.19.3087](https://dx.doi.org/10.3934/dcdsb.2014.19.3087).
- 441 [19] D. L. DeAngelis, Wei-Ming Ni and B. Zhang, Effects of diffusion on total biomass in heterogeneous
442 continuous and discrete-patch systems, *Theoretical Ecology*, 9 (2016), 443-453. [http://doi10.1007/](https://doi.org/10.1007/s12080-016-0302-3)
443 [s12080-016-0302-3](https://doi.org/10.1007/s12080-016-0302-3).
- 444 [20] B. Elbetch, T. Benzekri, D. Massart and T. Sari, The multi-patch logistic equation, *Discrete and Continuous*
445 *Dynamical System series B*, 26 (12) (2020), 6405-6424. [http://dx.doi.org/10.3934/dcdsb.2021025](https://dx.doi.org/10.3934/dcdsb.2021025)
- 446 [21] B. Elbetch, T. Benzekri, D. Massart and T. Sari; The multi-patch logistic equation with asymmetric
447 migration, *Rev. Integr. Temas Mat.*, 40, No. 1, 25-57 (2022). [http://doi10.18273/revint.](https://doi.org/10.18273/revint.v40n1-212022002)
448 [v40n1-212022002](https://doi.org/10.18273/revint.v40n1-212022002)
- 449 [22] B. Elbetch, Effect of dispersal in Two-patch environment with Richards growth on population dynamics, *J.*
450 *Innov. Appl. Math. Comput. Sci.* 2(3) (2022), 41-68. n2t.net/ark:/49935/jiamcs.v2i3.47
- 451 [23] B. Elbetch and A. Moussaoui. Nonlinear diffusion in the multi-patch logistic model. *Journal of Mathematical*
452 *Biology* 87:1, (2023) <https://doi.org/10.1007/s00285-023-01936-2>
- 453 [24] B. Elbetch, Effect of dispersal in single-species discrete diffusion systems with source-sink patches, *Mathe-*
454 *matica Applicanda*, Vol. 51 (1) 2023, p. 51-97 [doi:10.14708/ma.v51i1.7161](https://doi.org/10.14708/ma.v51i1.7161)
- 455 [25] B. Elbetch. On the effect of density-dependent dispersal on the global dynamics of population. *Annals of*
456 *Mathematical Sciences and Applications*, Volume 9, Number 2, 341-364, 2024.
- 457 [26] B. Elbetch. Effects of rapid population growth on total biomass in Multi-patch environment. *Differential*
458 *Equations and Applications*, Volume 15, Number 4 (2023), 323-359
- 459 [27] B. Elbetch. Generalized logistic equation on Networks. *Comptes Rendus. Mathématique*, Tome 361 (2023),
460 pp. 911-934. doi : 10.5802/crmath.460
- 461 [28] B. Elbetch, Influence of dispersal asymmetry on total biomass in two-patch environment with generalized
462 growth rate, *JOURNAL OF OPTIMIZATION, DIFFERENTIAL EQUATIONS AND THEIR APPLICA-*
463 *TIONS (JODEA)* Volume 32, Issue 2, December 2024, pp. 16-40, DOI 10.15421/142407
- 464 [29] B. Elbetch, Generalized Coupled Source-Sink Models, 2023 <https://hal.science/hal-04167884>
- 465 [30] B. Elbetch, A. Moussaoui, P. Auger, Increase maximum economic yield in a patchy environment, *Journal of*
466 *Mathematical Biology* (2025) 90:14 <https://doi.org/10.1007/s00285-024-02178-6>.
- 467 [31] B. Elbetch, A. Moussaoui, Enhancing maximum sustainable yield in a patchy prey-predator environment,
468 *Ecological Complexity* 60 (2024) 101107.
- 469 [32] B. Elbetch, A. Moussaoui, P. Auger. Increase Maximum Sustainable Yield in Gradostat, *International Journal*
470 *of Biomathematics*, <https://doi.org/10.1142/S1793524525500032>
- 471 [33] B. Elbetch, A. Moussaoui, IS IT POSSIBLE TO INCREASE MAXIMUM SUSTAINABLE YIELD IN A
472 MULTI-PATCH SCHAEFER MODEL?. 2024. <https://hal.science/hal-04778559>
- 473 [34] H. I. Freedman, *Deterministic Mathematical Models in Population Ecology*, Marcel Dekker, New York,
474 1980.
- 475 [35] H. I. Freedman, B. Rai and P. Waltman, Mathematical Models of Population Interactions with Dispersal
476 II: Differential Survival in a Change of Habitat, *Journal of Mathematical Analysis and Applications*, 115
477 (1986), 140-154. [https://doi.org/10.1016/0022-247X\(86\)90029-6](https://doi.org/10.1016/0022-247X(86)90029-6).
- 478 [36] H. I. Freedman and P. Waltman, Mathematical Models of Population Interactions with Dispersal I: Stability
479 of two habitats with and without a predator, *SIAM Journal on Applied Mathematics*, 32 (1977), 631-648.
480 [http://dx.doi.org/10.1137/0132052](https://dx.doi.org/10.1137/0132052).

- 481 [37] H. I. Freedman, Y. Takeuchi, Global stability and predator dynamics in a model of prey dispersal in a patchy
 482 environment. *Non linear Anal., Theory Methods Appl* 13(1989), 993-1002.
- 483 [38] D. Gao , How does dispersal affect the infection size?, *SIAM J. Appl. Math.* 80 (2020), No. 5, 2144-2169.
 484 doi:10.1137/19M130652X
- 485 [39] D. Gao and S. Ruan, A multipatch malaria model with logistic growth, *SIAM Journal on Applied Mathemat-*
 486 *ics*, Vol. 72, No. 3 (2012), pp. 819-841. <http://doi.10.1137/110850761>.
- 487 [40] D. Gao and Dong C.P., Fast diffusion inhibits disease outbreak, *Proc. Am. Math. Soc.* 148 (2020), No. 4,
 488 1709-1722. doi:10.1090/proc/14868
- 489 [41] H. Guo, M. Y. Li, and Z. Shuai, Global stability of the endemic equilibrium of multigroup SIR epidemic
 490 models, *Canad. Appl. Math. Quart.*, 14 (2006), pp. 259-284.
- 491 [42] Gurney, W. S. C., Nisbet, R. M.: The regulation of inhomogeneous populations. *J. Theor. Biol.* 52, 441-457
 492 (1975)
- 493 [43] R. Hilborn, F. Michel, G. A. DeLeo, Integrating marine protected areas with catch regulation. *Canadian*
 494 *journal of Fisheries and Aquatic Sciences*, 63 (2006), 642-649.
- 495 [44] R. D. Holt, Population dynamics in two patch environments: some anomalous consequences of an optimal
 496 habitat distribution, *Theoretical Population Biology*, 28 (1985), 181-201. [http://dx.doi.org/10.1016/](http://dx.doi.org/10.1016/0040-5809(85)90027-9)
 497 [0040-5809\(85\)90027-9](http://dx.doi.org/10.1016/0040-5809(85)90027-9).
- 498 [45] Y. Kuang and Y. Takeuchi, Predator-prey dynamics in models of prey dispersal in two-patch environments,
 499 *Math. Biosci.* 120 (1994) 77-98.
- 500 [46] G. Katriel. Dispersal-induced growth in a time-periodic environment. *J. Math. Biol.* 85, 24 (2022).
 501 <https://doi.org/10.1007/s00285-022-01791-7>
- 502 [47] C. Lobry, T. Sari and S. Touhami, On Tykhonov's theorem for convergence of solutions of slow and
 503 fast systems, *Electron. J. Differential Equations*, 19 (1998), 1-22. [http://refhub.elsevier.com/](http://refhub.elsevier.com/S0040-5809(15)00102-1/sbref11)
 504 [S0040-5809\(15\)00102-1/sbref11](http://refhub.elsevier.com/S0040-5809(15)00102-1/sbref11).
- 505 [48] T. Legovic, J. Klanjscek, S. Gecek, Maximum sustainable yields and species extinction in ecosystems, *Eco-*
 506 *logical Modelling*, 221, (2011), 1569- 1574.
- 507 [49] Y. Li, H.Gao, C. Sun, A. Sedki, Asymptotic stability problem of predator-prey system with linear diffusion,
 508 *Applied Mathematics and Nonlinear Sciences (aop) (aop)* 1-12 [http://doi:10.2478/amns.2022.1.](http://doi:10.2478/amns.2022.1.00022)
 509 [00022](http://doi:10.2478/amns.2022.1.00022)
- 510 [50] A. Moussaoui, M.Bensenane, P. Auger, Alassane Bah, On the optimal size and number of reserves in a
 511 multi-site fishery model. *Journal of Biological Systems*, 22 (2014), 1-17.
- 512 [51] A. Moussaoui, M.Bensenane, P. Auger, Alassane Bah, On the optimal size and number of reserves in a
 513 multi-site fishery model. *Canadian journal of Fisheries and Aquatic Sciences*, 67 (2010), 296-303.
- 514 [52] A. Moussaoui, P.Auger, C. Lett, Optimal number of sites in multi-site fisheries with fish stock dependent
 515 migrations. *Mathematical Biosciences and Engineering* , 8 (2011), 769-783.
- 516 [53] A. Moussaoui, P. Auger, B. Elbetch, Increase in Maximum Sustainable Yield in Multi-patch Rosenzweig-
 517 Macarthur predator-prey model, *Math. Model. Nat. Phenom.*, [https://doi.org/10.1051/mmnp/](https://doi.org/10.1051/mmnp/2025004)
 518 [2025004](https://doi.org/10.1051/mmnp/2025004)
- 519 [54] J.D. Murray. *Mathematical Biology I. An Introduction*. Springer-Verlag, New York, (2002).
- 520 [55] F.J. RICHARDS, *A Flexible Growth Function for Empirical Use*. *Journal of Experimental Botany*, 10 (29),
 521 290-300 (1959). DOI: 10.1093/jxb/10.2.290
- 522 [56] M.B. Schaefer, Some considerations of population dynamics and economics in relation to the management
 523 of the commercial marine fisheries. *J. Fish. Res. Board Canada.* 14(5), (1957), 669-681.
- 524 [57] H. L. Smith and P. Waltman, The Theory of the Chemostat, *Cambridge studies in mathematical biology*,
 525 1995.
- 526 [58] Y. Takeuchi, Cooperative systems theory and global stability of diffusion models, *Acta Applicandae Mathe-*
 527 *maticae*, 14 (1989), 49-57. https://doi.org/10.1007/978-94-009-2358-4_6.
- 528 [59] A. N. Tikhonov, Systems of differential equations containing small parameters in the derivatives, *Mat. Sb.*
 529 *(N.S.)*, 31 (1952), 575-586. [http://refhub.elsevier.com/S0040-5809\(15\)00102-1/sbref18](http://refhub.elsevier.com/S0040-5809(15)00102-1/sbref18).
- 530 [60] W. R. Wasow, Asymptotic Expansions for Ordinary Differential Equations, *Robert E. Krieger Publishing*
 531 *Company*, Huntington, NY, 1976.
- 532 [61] H. Wu, Y. Wang, Y. Li and D. L. DeAngelis, Dispersal asymmetry in a two-patch system with source-sink
 533 populations. *Theoretical Population Biology* (2019), <https://doi.org/10.1016/j.tpb.2019.11.004>
- 534 *E-mail address: elbetchbilal@gmail.com, ali.moussaoui@univ-tlemcen.dz*